Cancer Research

Targeting Mitochondria with Avocatin B Induces Selective Leukemia Cell Death

Eric A. Lee[1], Leonard Angka[1], Sarah-Grace Rota[1], Thomas Hanlon[1], Andrew Mitchell[2], Rose Hurren[3], Xiao Ming Wang[3], Marcela Gronda[3], Ezel Boyaci[4], Barbara Bojko[4], Mark Minden[3], Shrivani Sriskanthadevan[3], Alessandro Datti[5,6], Jeffery L. Wrana[5], Andrea Edginton[1], Janusz Pawliszyn[4], Jamie W. Joseph[1], Joe Quadrilatero[2], Aaron D. Schimmer[3], and Paul A. Spagnuolo[1]

Abstract

Treatment regimens for acute myeloid leukemia (AML) continue to offer weak clinical outcomes. Through a high-throughput cell-based screen, we identified avocatin B, a lipid derived from avocado fruit, as a novel compound with cytotoxic activity in AML. Avocatin B reduced human primary AML cell viability without effect on normal peripheral blood stem cells. Functional stem cell assays demonstrated selectivity toward AML progenitor and stem cells without effects on normal hematopoietic stem cells. Mechanistic investigations indicated that cytotoxicity relied on mitochondrial localization, as cells lacking functional mitochondria or CPT1, the enzyme that facilitates mitochondria lipid transport, were insensitive to avocatin B. Furthermore, avocatin B inhibited fatty acid oxidation and decreased NADPH levels, resulting in ROS-dependent leukemia cell death characterized by the release of mitochondrial proteins, apoptosis-inducing factor, and cytochrome *c*. This study reveals a novel strategy for selective leukemia cell eradication based on a specific difference in mitochondrial function. *Cancer Res; 75(12); 2478–88. ©2015 AACR.*

Introduction

Leukemia and leukemia stem cells (LSC) possess several mitochondrial features that distinguish them from normal hematopoietic cells. Compared with normal cells, leukemia cells contain greater mitochondrial mass, have higher rates of oxidative phosphorylation (1), and depend on fatty acid oxidation for survival (2). Together, these altered mitochondrial characteristics may make drugs that target mitochondria potentially useful for the eradication of leukemia cells.

Acute myeloid leukemia (AML) is a devastating disease characterized by the accumulation of malignant myeloid precursors that fail to terminally differentiate (3). Patients diagnosed with AML are faced with poor disease prognosis. In adults (>65), 2-year survival rates are less than 10% (4). The suboptimal quality of current therapy is, in part, attributed to the inability of current drugs to target and eliminate LSCs. Thus, new therapeutic strategies that target both the bulk and LSC populations are needed to improve AML patient outcomes.

To identify novel AML therapeutics, we screened a natural health product library ($n = 800$) for compounds that induce death of TEX leukemia cells, an AML cell line with features of LSCs (1, 5, 6). From this screen, we identified avocatin B, a lipid-derived from avocados, as a novel anti-AML compound.

Materials and Methods

Cell culture

Leukemia (OCI-AML2) cells were cultured in Iscove's Modified Dulbecco's Medium (IMDM; Life Technologies) supplemented with 10% fetal bovine serum (FBS; Seradigm) and antibiotics (100 U/mL of streptomycin and 100 μg/mL of penicillin; Sigma Chemical). TEX leukemia cells were cultured in 15% FBS, antibiotics, 2 mmol/L L-glutamine (Sigma Chemical), 20 ng/mL stem cell factor and 2 ng/mL IL3 (Peprotech). Primary human samples (fresh and frozen) were obtained from the peripheral blood of AML patients who had at least 80% malignant cells among the mononuclear cells and cultured at 37°C in IMDM, 20% FBS, and antibiotics (see Supplementary Tables S2 and S3 for clinical parameters). Normal G-CSF-mobilized peripheral blood mononuclear cells were obtained from volunteers donating peripheral blood stem cells (PBSC) for allotransplant and were cultured similar to the primary AML samples. The collection and use of human tissue for this study was approved by the local ethics review board (University Health Network, Toronto, ON, Canada; University of Waterloo, Waterloo, ON, Canada).

Cell growth and viability

Cell growth and viability was measured using the 3-(4,5-dimethylthiazol-2-yl)-5-(3-carboxymethoxyphenyl)-2-(4-sulfophenyl)-2H-tetrazolium inner salt (MTS) reduction assay

[1]School of Pharmacy, University of Waterloo, Kitchener, Ontario, Canada. [2]Department of Kinesiology, University of Waterloo, Waterloo, Ontario, Canada. [3]Princess Margaret Cancer Center, Ontario Cancer Institute, Toronto, Ontario, Canada. [4]Department of Chemistry, University of Waterloo, Waterloo, Ontario, Canada. [5]SMART Laboratory for High-Throughput Screening Programs, Samuel Lunenfeld Research Institute, Mount Sinai Hospital, Toronto, Ontario, Canada. [6]Department of Agricultural, Food and Environmental Sciences, University of Perugia, Perugia, Italy.

Note: Supplementary data for this article are available at Cancer Research Online (http://cancerres.aacrjournals.org/).

Corresponding Author: Paul A. Spagnuolo, School of Pharmacy, Health Science Campus, Room 4002, University of Waterloo, 10A Victoria Street South, Kitchener, ON N2G 1C5. Phone: 519-888-4567, ext. 21372; Fax: 519-888-7910; E-mail: paul.spagnuolo@uwaterloo.ca

doi: 10.1158/0008-5472.CAN-14-2676

(Promega) according to the manufacturer's protocol and as previously described (7). Cells were seeded in 96-well plates, treated with drug for 72 hours, and optical density (OD) was measured at 490 nm. Cell viability was also assessed by the Trypan blue exclusion assay and by Annexin V and propidium iodide (PI) staining (Biovision), as previously described (7).

Functional stem cell assays

Clonogenic growth assays with primary AML and normal hematopoietic stem cells were performed, as previously described (7). Briefly, $CD34^+$ bone marrow–derived normal stem cells (STEMCELL Technologies) or AML mononuclear cells from patients with >80% blasts in their peripheral blood (4×10^5 cells/mL) were treated with vehicle control or increasing concentrations of avocatin B and plated in duplicate by volume at 10^5 cells/mL per 35-mm dish (Nunclon) in MethoCult GF H4434 medium (STEMCELL Technologies) containing 1% methylcellulose in IMDM, 30% FBS, 1% bovine serum albumin (BSA), 3 U/mL recombinant human erythropoietin, 10^{-4} mol/L 2-mercaptoethanol (2ME), 2 mmol/L L-glutamine, 50 ng/mL recombinant human stem cell factor, 10 ng/mL recombinant human granulocyte macrophage-colony-stimulating factor, and 10 ng/mL recombinant human IL3. After 7 to 10 days of incubation at 37°C with 5% CO_2 and 95% humidity, the number of colonies were counted on an inverted microscope with a cluster of 10 or more cells counted as one leukemic colony and 50 or more cells counted as a normal colony similar to previously described methods (1, 8).

Mouse xenotransplant assays were performed as previously described (1, 9). Briefly, AML patient cells were treated with 3 μmol/L avocatin B or dimethyl sulfoxide (DMSO; as a control) for 48 hours *in vitro*. Next, these cells were transplanted into femurs of sublethally irradiated, CD122-treated NOD/SCID mice and following a 6-week engraftment period, mice were sacrificed, femurs excised, bone marrow flushed, and the presence of human myeloid cells ($CD45^+/CD33^+/CD19^-$) was detected by flow cytometry. All animal studies were carried out according to the regulations of the Canadian Council on Animal Care and with the approval of the University Health Network, Animal Care Committee.

High-throughput screen

A high-throughput screen of a natural product library ($n = 800$; Microsource Discovery Systems Inc.) was performed as previously described (1, 7). Briefly, TEX leukemia cells (1.5×10^4/well) were seeded in 96-well polystyrene tissue culture plates. After seeding, cells were treated with aliquots (10 μmol/L final concentration) of the chemical library with a final DMSO concentration no greater than 0.05%. After 72 hours, cell proliferation and viability were measured by the MTS assay.

Protein and mRNA detection

Western blotting was performed as previously described (10). Briefly, whole-cell lysates were prepared from treated cells, heated for 5 minutes at 95°C, and subjected to gel electrophoresis on 7.5% to 15% SDS-PAGE at 150 V for 85 minutes. The samples were then transferred at 25 V for 45 minutes to a polyvinylidene difluoride membrane and blocked with 5% BSA in Tris-buffered saline-tween (TBS-T) for 1 hour. The membrane was incubated overnight at 4°C with the primary antibody, poly(ADP) ribose polymerase (PARP)a (1:1,500; Cell Signaling Technology), ANT (1:1,000; Santa Cruz Biotechnology), ND1 (1:10,000; Santa Cruz Biotechnology), or α-tubulin (loading control; 1:5,000; Santa Cruz Biotechnology). Membranes were then washed and incubated with the appropriate secondary antibody (1:10,000) for 1 hour at room temperature. Enhanced chemiluminescence (ECL) was used to detect proteins according to the manufacturer's instructions (GE Healthcare) and luminescence was captured using the Kodak Image Station 4000MM Pro and analyzed with a Kodak Molecular Imaging Software Version 5.0.1.27.

Quantitative PCR was performed as previously described (6) in triplicate using an ABI 7900 Sequence Detection System (Applied Biosystems) with 5 ng of RNA equivalent cDNA, SYBR Green PCR Master Mix (Applied Biosystems), and 400 nmol/L of CPT1-specific primers (forward: 5′-TCGTCACCTCTTCTGCCTTT-3′, reverse: 5′-ACACACCATAGCCGTCATCA-3′). Relative mRNA expression was determined using the $\Delta\Delta C_T$ method as previously described (6).

Assessment of fatty acid oxidation and mitochondrial respiration

Measurement of oxygen consumption rates (OCR) was performed using a Seahorse XF24 extracellular flux analyzer (Seahorse Bioscience). TEX cells were cultured in α-minimum essential medium (Life Technologies) containing 1% FBS and plated at 1×10^5 cells per well in poly-L-lysine (Sigma Chemical)–coated XF24 plates. Cells were incubated with etomoxir (100 μmol/L; Sigma Chemical) or vehicle control for 30 minutes at 37°C in a humidified atmosphere containing 5% CO_2. Next, palmitate (175 μmol/L; Seahorse Bioscience) or avocatin B (10 μmol/L) was added and immediately transferred to the XF24 analyzer. Oxidation of exogenous fatty acids was determined by measuring mitochondrial respiration through sequential injection of 5 μmol/L (final concentration) oligomycin, an ATP synthase inhibitor (Millipore), 5 μmol/L CCCP, a hydrogen ion ionophore (Sigma Chemical), and 5 μmol/L rotenone (Millipore)/5 μmol/L antimycin A, which inhibit complex III activity (Sigma Chemical). Fatty acid oxidation was determined by the change in oxygen consumption following oligomycin and CCCP treatment and prior to antimycin and rotenone treatment, according to the manufacturer's protocol and as described by Abe and colleagues (11). Data were analyzed with XF software (Seahorse Bioscience).

ROS, NADH, NADPH, and GSH detection

Reactive oxygen species (ROS) were detected using 2′,7′dichlorohydrofluorescein-diacetate (DCFH-DA; Sigma Chemical) and dihyodroethidium (DHE; Sigma Chemical). DCFH-DA is hydrolyzed by intracellular esterase to produce a nonfluorescent DCFH product. It can then be oxidized by ROS and other oxidizing species to produce a highly fluorescent DCF product (12). DHE is a superoxide indicator that, upon contact with superoxide anions, produces the fluorescent product 2-hydroxyethidium (13). Following drug treatment, TEX cells (5×10^5) were collected and washed in PBS (Sigma-Aldrich). Cells were stained with 5 μmol/L (final concentration) DCFH-DA or 10 μmol/L DHE and allowed to incubate for 30 minutes in a humidified atmosphere containing 5% CO_2 at 37°C. Samples were then washed in PBS and ROS were measured by flow cytometry using the Guava EasyCyte 8HT (Millipore). Data were analyzed with GuavaSoft 2.5 software (Millipore).

Nicotinamide adenine dinucleotide phosphate (NADPH), nicotinamide adenine dinucleotide (NAD), and glutathione (GSH) were measured by commercially available fluorimetric kits (AAT

Bioquest), according to the manufacturers' protocol, following incubation of increasing duration with avocatin B (10 μmol/L). For NADPH studies, cells were also incubated with palmitate (175 μmol/L) in the presence or absence of etomoxir (100 μmol/L). For NADH and GSH studies, cells were incubated in the presence of palmitate and *N*-acetylcysteine (NAC; 1 mmol/L), respectively. Data are presented as a percent NAD, NADPH, or GSH compared with control-treated cells ± SD.

Liquid chromatography/mass spectroscopy

Avocatin B's presence in mitochondria and cytosolic fractions was detected using thin film solid-phase microextraction (TF-SPME; Professional Analytical System Technology) followed by liquid chromatography–high resolution mass spectrometry analysis (LC/MS; Thermo Exactive Orbitrap mass spectrometer; Thermo Scientific; refs. 14, 15). TEX cells were treated with avocatin B or a vehicle control for 1 hour, as performed for the Seahorse Bioanalyzer experiments (i.e., assessment of fatty acid oxidation), and cytosolic and mitochondrial fractions were then isolated, as previously described (16). Fraction purity was determined by Western blot analysis for the mitochondrial-specific protein ND1 (i.e., complex 1). Next, samples were prepared by TF-SPME and then subjected to LC/MS analysis. For detailed methods on sample preparation, standardization, and calibration, please refer to the Supplementary Methods.

Apoptosis determination

Caspase activation, PARP cleavage, Annexin V/PI, and DNA fragmentation assays were performed, as previously described (10). Release of proapoptotic mitochondrial proteins cytochrome *c* and apoptosis-inducing factor (AIF) were assessed using a flow cytometry–based assay, as previously described (17, 18) and these assays are further detailed in the Supplementary Methods.

Statistical analysis

Unless otherwise stated, the results are presented as mean ± SD. Data were analyzed using GraphPad Prism 4.0 (GraphPad Software). $P \leq 0.05$ was accepted as being statistically significant.

Results

A high-throughput screen for novel anti-AML compounds identifies avocatin B

To identify novel compounds with anti-AML activity, we screened a commercially available natural health products–specific library against TEX leukemia cells. These cells possess several LSC properties, such as marrow repopulation and self-renewal (1, 5, 6, 19). The compound that imparted the greatest reduction in viability was avocatin B (Fig. 1A; arrow indicates avocatin B). Avocatin B is a 1:1 mixture of two 17-carbon lipids derived from avocados and belongs to a family of structurally related lipids (Fig. 1A insert: avocatin B's structure; refs. 20, 21). We tested four avocatin lipid analogues and determined that avocatin B was the most cytotoxic (EC_{50}: 1.5 ± 0.75 μmol/L; Supplementary Fig. S1 and Table S1).

Avocatin B's selectivity toward leukemia cells was validated in primary AML samples and in PBSCs isolated from G-CSF–stimulated healthy donors. Avocatin B, at concentrations as high as 20 μmol/L, had no effect on the viability of normal PBSCs ($n = 4$). In contrast, avocatin B reduced the viability of primary AML patient cells ($n = 6$) with an EC_{50} of 3.9 ± 2.5 μmol/L, which is similar to other recently identified compounds with anti-AML activity (Fig. 1B; see Supplementary Table S2 for patient sample characteristics; refs. 1, 8, 9, 22).

Avocatin B is selectively toxic toward leukemia progenitor and stem cells

Given the selectivity toward AML patient samples over normal hematopoietic cells, we next assessed avocatin B's effects on functionally defined subsets of primitive human AML and normal cell populations. Adding avocatin B (3 μmol/L) into the culture medium reduced clonogenic growth of AML patient cells ($n = 3$; Supplementary Table S3 for patient characteristics). In contrast, there was no effect on normal cells ($n = 3$; Fig. 1C, left). In addition, treatment of primary AML cells with avocatin B (3 μmol/L) reduced their ability to engraft in the marrow of immune-deficient mice (Fig. 1C, right). Taken together, avocatin B selectively targets primitive leukemia cells.

Avocatin B induces mitochondria-mediated apoptosis

We next assessed the mode of avocatin B–induced leukemia cell death. Externalization of phosphatidylserine, an early marker of apoptosis detected by Annexin V, was observed by flow cytometry in live cells (i.e., Annexin V^+/PI^-) treated with avocatin B (Fig. 2A; $F_{3,7} = 19.09$; $P < 0.05$; see Supplementary Fig. S2 for raw data). This coincided with the occurrence of DNA fragmentation (Fig. 2B; $F_{4,14} = 171.4$; $P < 0.001$), caspase activation (Fig. 2C; $F_{3,16} = 69.56$; $P < 0.001$), and PARP cleavage (Fig. 2D), as measured by cell-cycle analysis (see Supplementary Fig. S3 for raw data), a caspase activation assay, and Western blotting, respectively.

To test whether death was dependent on caspase enzymes, we coincubated avocatin B with the pan-caspase inhibitor Z-VAD-FMK or the caspase-3–specific inhibitor QVD-OPh for 72 hours. Both inhibitors only slightly protected cells from avocatin B–induced death ($F_{4,9} = 2.714$; $P < 0.01$; Fig. 2E). Because cell death can occur independent of caspase enzymes through the release of mitochondria-localized proteins, such as AIF, we tested for the presence of AIF in cytosolic fractions of avocatin B–treated TEX cells. However, given that AIF release involves mitochondrial outer membrane permeability and that we detected caspase activation, we also simultaneously tested for the presence of cytochrome *c*, which activates caspase enzymes following its release from the mitochondrial intermembrane space. Cells treated with avocatin B showed an increase in cytoplasmic concentrations of AIF (Fig. 2F; $F_{4,20} = 8.211$; $P < 0.001$) and cytochrome *c* (Fig. 2F; $F_{4,20} = 13.57$; $P < 0.001$). Therefore, avocatin B–induced apoptotic death is characterized by the release of the mitochondrial proteins AIF and cytochrome *c*; however, AIF is likely the key mediator, as death occurred in the presence of caspase inhibitors. Future studies would be needed to confirm the functional importance of AIF in avocatin B–induced death.

Avocatin B inhibits fatty acid oxidation

Apoptosis was characterized by the release of mitochondrial proteins following avocatin B treatment. Because avocatin B contains 17-carbon lipids and lipids of that size can enter the mitochondria and undergo fatty acid oxidation after they have been processed by carnitine palmitoyltransferase 1 (CPT1), we evaluated the impact of avocatin B on fatty acid oxidation. Fatty acid oxidation produces acetyl-CoA, which enters the TCA cycle to produce

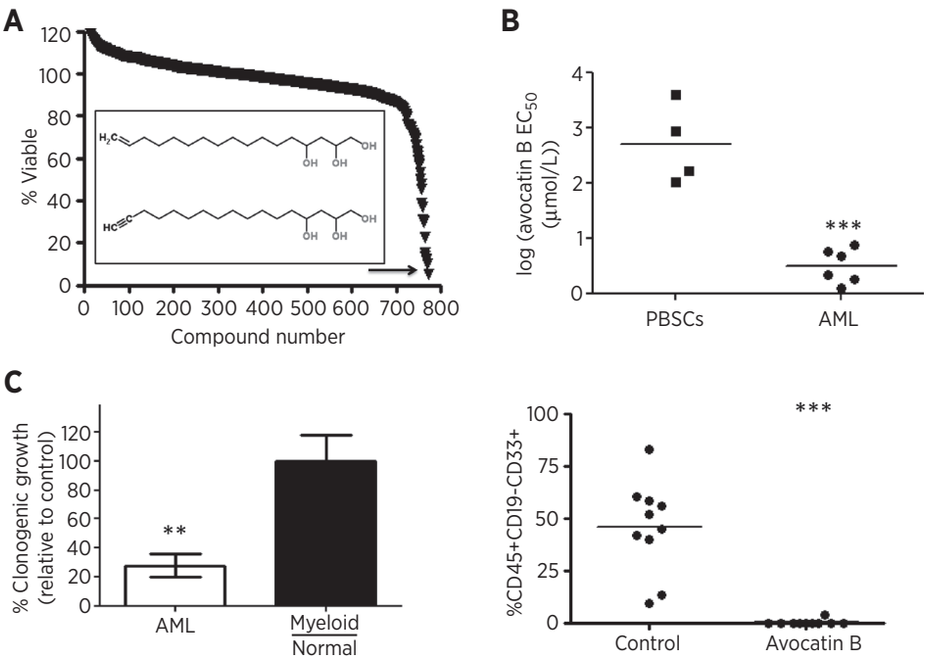

Figure 1.

Avocatin B is selectively toxic toward AML cells. A, left, a screen of a natural health product library identified avocatin B as the most potent compound at reducing TEX leukemia cell viability. Cells were incubated with compounds for 72 hours and cell growth and viability were measured by the MTS assay. Arrow, avocatin B. Inset, avocatin B's structure (21). B, avocatin B's activity was tested in PBSCs ($n = 4$) isolated from G-CSF–stimulated donors or cells isolated from AML patients ($n = 6$). Primary cells were treated with increasing avocatin B concentrations for 72 hours and viability was measured by the Annexin V/PI assay and flow cytometry. Data, $\log_{10}$ EC_{50} values. C, left, primary AML ($n = 3$) and normal ($n = 3$) cells were cultured with avocatin B (3 μmol/L) for 7 to 14 days and clonogenic growth was assessed by enumerating colonies as described in Materials and Methods. Data, percentage of clonogenic growth compared with control ± SEM, similar to previously described (1). Experiments were performed twice in triplicate. Right, AML cells from one patient were treated with avocatin B (3 μmol/L) or a vehicle control for 48 hours and then intrafemorally injected into sublethally irradiated, CD122-treated NOD/SCID mice ($n = 10$/group). After 6 weeks, human AML cells ($CD45^+/CD19^-/CD33^+$) in mouse bone marrow were detected by flow cytometry. **, $P < 0.01$; ***, $P < 0.001$.

NADH, which fuels oxidative phosphorylation, and NADPH, which is an important cofactor that participates in catabolic processes during cell proliferation (23) and can also regenerate the oxidized form of GSH (e.g., GSSG) to produce reduced GSH—an important intracellular and mitochondrial antioxidant (Fig. 3A; refs. 24, 25). To test the effects of avocatin B on fatty acid oxidation, we measured mitochondrial bioenergetics of TEX cells preincubated with avocatin B or palmitate in the absence or presence of etomoxir by measuring the change in maximum oxygen consumption following oligomycin and CCCP treatment and prior to the addition of antimycin and rotenone, as previously described (11). As expected, treatment with palmitate increased the OCR, consistent with oxidation of exogenous fatty acid substrates and this increase was blocked by treatment with etomoxir, a CPT1 inhibitor (Fig. 3B and C). Similarly, avocatin B reduced palmitate oxidation, demonstrating that avocatin B inhibits the oxidation of exogenous fatty acids (Fig. 3B and C; $F_{5,17} = 40.83$; $P < 0.05$; arrows indicate when oligomycin, CCCP, and antimycin/rotenone were added). Future studies are needed to further determine the nature of CPT1's preference for avocatin B over palmitate.

Inhibiting fatty acid oxidation results in reduced NAD, NADPH, and GSH and elevated ROS

Inhibiting fatty acid oxidation can decrease NAD, NADPH, and GSH and subsequently decrease antioxidant capabilities (26). Thus, we tested the effect of avocatin B on NAD, NADPH, and GSH levels in leukemia cells. Avocatin B (10 μmol/L), similar to etomoxir (100 μmol/L), decreased NADPH, an effect that occurred even in the presence of palmitate (175 μmol/L; Fig. 4A; $F_{9,19} = 5.129$; $P < 0.05$). Similarly, avocatin B decreased NADH and GSH (Fig. 3D: NAD: $F_{3,11} = 5.145$; $P < 0.05$; Fig. 4B: GSH: $F_{4,14} = 188.9$; $P < 0.001$).

Inhibition of fatty acid oxidation can reduce NADPH and GSH, leading to reduced antioxidant capacity, elevated ROS, and cell death (26). ROS levels were tested in avocatin B–treated cells using DCFH-DA and DHE, which measure general oxidizing species such as ROS and superoxide, respectively. TEX or primary AML cells treated with avocatin B had a time-dependent increase in ROS levels as measured by DCFH-DA (Fig. 4C, left; $F_{5,11} = 176.7$; $P < 0.01$; see Supplementary Fig. S4 for histogram data) and DHE ($F_{5,11} = 36.75$; $P < 0.01$; Fig. 4C; see Supplementary Fig. S4 for histogram data). To test the importance of ROS in avocatin B–induced death, we coincubated cells with NAC and α-tocopherol (α-Toc). NAC can neutralize a number of oxidizing species, including ROS directly or indirectly through antioxidant regeneration [i.e., convert oxidized GSH (i.e., GSSG) to reduced GSH; GSH is decreased following NADPH depletion; ref. 26] and α-Toc is a lipid-based antioxidant that accumulates in organelle membranes, particularly mitochondria, to prevent lipid peroxyl radicals formed by ROS-induced membrane damage (27). Coincubation with NAC (Fig. 4D: $F_{3,7} = 70.55$, $P < 0.05$; Fig. 4E: $F_{3,10} = 70.55$, $P < 0.05$) or α-Toc (Fig. 4D; $F_{3,7} = 10.23$; $P < 0.05$)

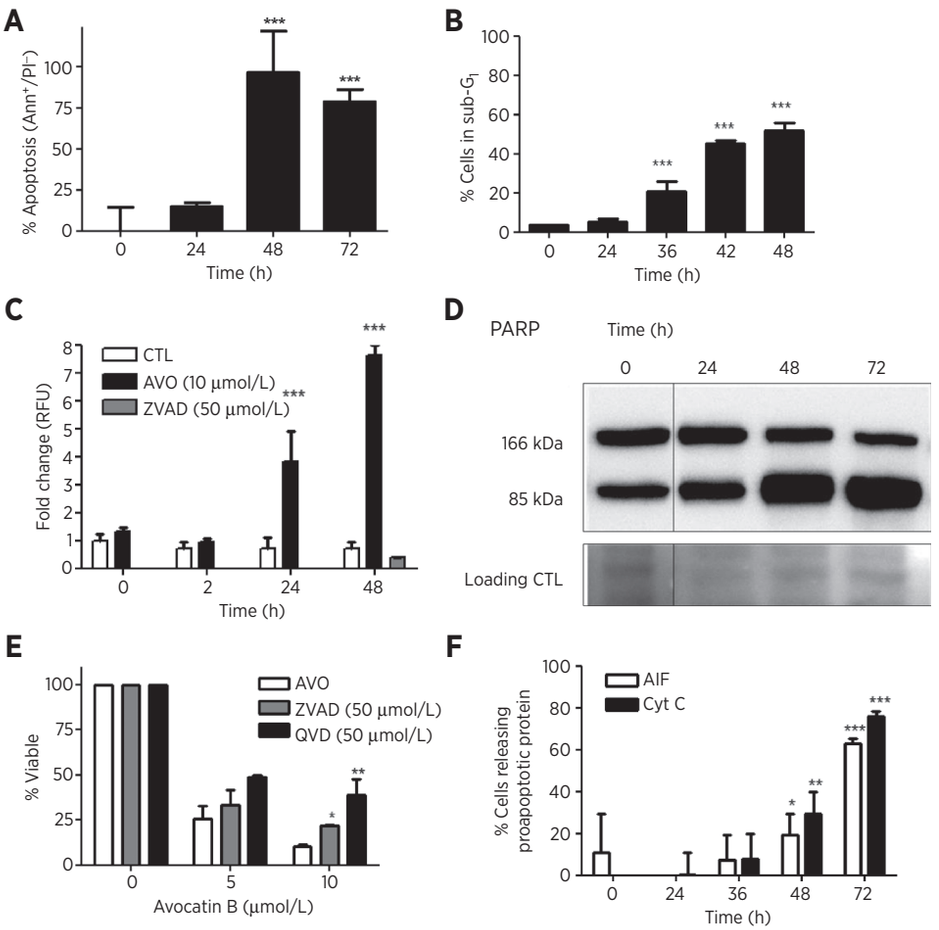

Figure 2.
Avocatin B induces mitochondria-mediated apoptosis. A and B, TEX cells were treated with 10 μmol/L avocatin B for increasing duration and phosphatidylserine exposure in live cells (i.e., apoptotic phenotype; ANN^+/PI^-; A) and DNA fragmentation (B) was measured by flow cytometry. Data, fold change in apoptotic phenotype and percentage of cells in sub-G_1 peak, respectively. C and D, TEX cells were treated with 10 μmol/L avocatin B for increasing duration and caspase-3 and -7 activation (C) and cleavage of PARP, a substrate of caspase-3, was measured by a commercially available activation assay and Western blotting (D), respectively. E, TEX cells were treated with 10 μmol/L avocatin B in the presence and absence of the pan-caspase inhibitor Z-VAD-FMK (ZVAD) or the caspase-3–specific inhibitor Q-VD-OPh (QVD). Viability was measured after a 72-hour incubation period by the MTS assay. Data, percentage change in viability compared with controls ± SD. F, TEX cells were treated with 10 μmol/L avocatin B for increasing duration and cytochrome *c* and AIF release was measured in cytoplasmic fractions by flow cytometry. Data, percentage of cells releasing cytochrome *c* or AIF ± SD. All experiments were performed three times in triplicate, and representative figures are shown. *, $P < 0.05$; **, $P < 0.01$; ***, $P < 0.001$.

abolished avocatin B–induced death. Daunorubicin was used as a negative control, as antioxidants do not protect against its cytotoxicity (28, 29). Finally, we coincubated cells with polyethylene glycol-superoxide dismutase (PEG-SOD), an antioxidant that reduces cellular concentrations of the superoxide anion. Coincubation with PEG-SOD similarly reduced ROS and blocked-avocatin B's activity (Supplementary Fig. S5). Together, these results demonstrate that avocatin B decreased levels of NAD, NADPH, and GSH and that ROS is functionally important for avocatin B's activity.

Mitochondria and CPT1 are functionally important for avocatin B-induced death

We demonstrated that avocatin B inhibits fatty acid oxidation and induces apoptosis characterized by the release of mitochondrial proteins cytochrome *c* and AIF. Because avocatin B is a lipid and leukemia cells possess mitochondrial and metabolic alterations that result in their dependence on fatty acid substrates for survival (2), we hypothesized that avocatin B's toxicity was related to its localization in mitochondria. To first test avocatin B's reliance on mitochondria for cytotoxicity, we generated leukemia cells lacking functional mitochondria by culturing Jurkat-T cells in media supplemented with 50 ng/mL of ethidium bromide, 100 mg/mL sodium pyruvate, and 50 μg/mL uridine, as previously described (30, 31). Following 60 days of passaging only live cells, the presence of mitochondria were tested by flow cytometry following 10-nonyl acridine orange (NAO) staining and by Western blotting for mitochondrial specific proteins ND1 and adenine nucleotide translocator (ANT). The significant reduction of mitochondria was confirmed, as cells cocultured in ethidium bromide containing media demonstrated a drastic reduction in NAO staining (Supplementary Fig. S6), absence of mitochondrial respiration (Supplementary Fig. S6), and a near absence of ND1 and ANT (Fig. 5A). Avocatin B's toxicity was abolished in cells lacking functional mitochondria (i.e., JURK-Rho(0) cells), as measured by the Annexin V/PI assay (Fig. 5B; $F_{2,12} = 6.509$; $P < 0.001$). Highlighting the utility of these cells in assessing mitochondrial participation in drug activity, we have previously shown that cells lacking mitochondria were equally sensitive to their mitochondria containing controls when subjected to a compound that activates mitochondria-independent, calpain-mediated apoptosis (10).

To directly examine whether avocatin B accumulated into mitochondria, LC/MS was performed on mitochondria and cytosolic fractions of avocatin B or vehicle control–treated TEX cells. Fraction purity was confirmed by Western blot analysis of the mitochondria-specific protein ND1 (Fig. 5C; Supplementary Fig. S8). Avocatin B was detected in mitochondrial and cytosolic fractions of avocatin B–treated TEX cells (Fig. 5D). Two peaks [with a mass/charge (m/z) ratio of 285.24242 and 287.25807] were detected, which reflect the nature of avocatin B's two-lipid composition. Importantly, retention times (min)

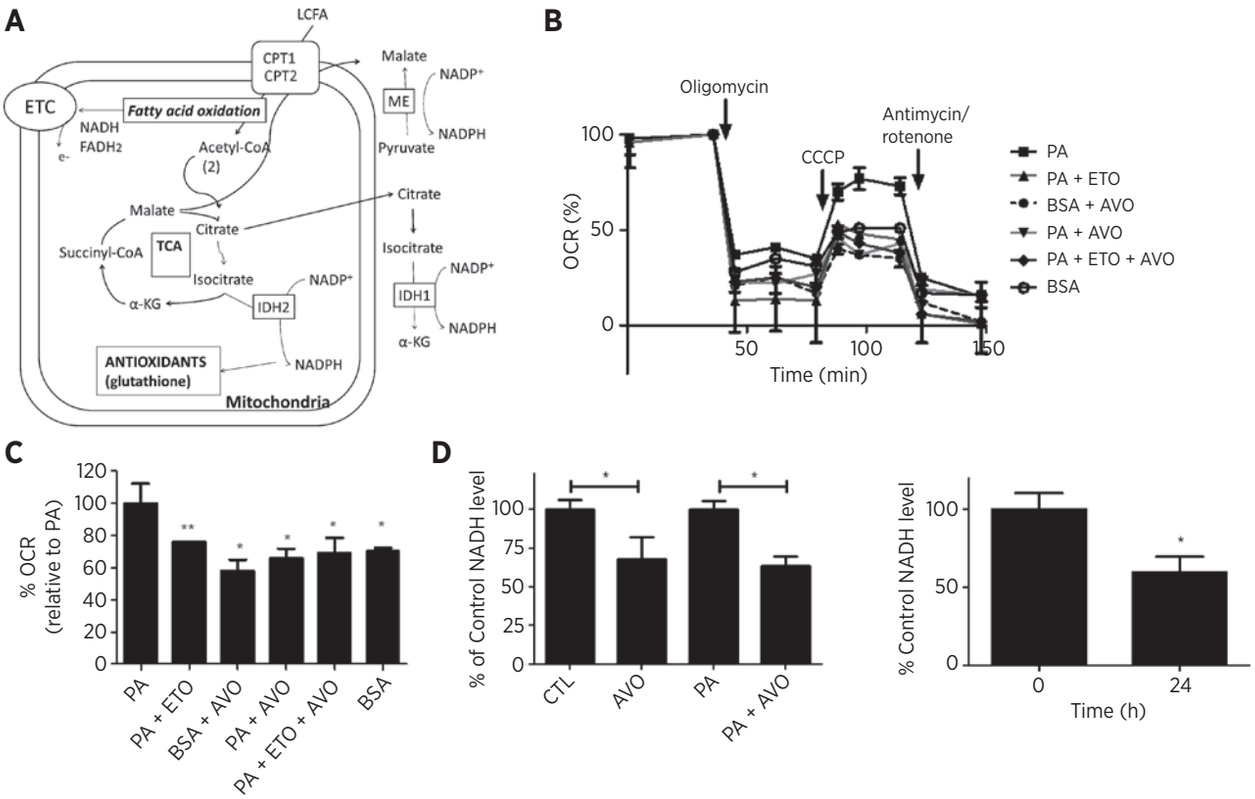

Figure 3.
Avocatin B inhibits fatty acid oxidation, resulting in decreased levels of NADH. A, illustration of fatty acid oxidation in mitochondria. Long-chain fatty acids (LCFA) enter the mitochondria via CPT1 for fatty acid oxidation to yield NADH and acetyl-CoA. Acetyl-CoA enters the TCA cycle to generate NADPH. ME, malic enzyme; IDH, isocitrate dehydrogenase; α-KG, α-ketoglutarate. B, oxidation of exogenous fatty acids was assessed by measuring the OCR in TEX cells treated with palmitate (175 μmol/L), avocatin B (10 μmol/L), avocatin B, and palmitate or palmitate and etomoxir (100 μmol/L). Arrows, the time when oligomycin, CCCP, and antimycin/rotenone were added to the cells. Effects on fatty acid oxidation were measured with the Seahorse Bioanalyzer and quantified (C) by peak area after oligomycin and CCCP treatment, as described by the manufacturer's protocol and detailed in Materials and Methods. Data, percentage of OCR compared with palmitate-treated cells ± SD. BSA was also used as a control. D, NADH was measured in TEX cells (left; $t = 3$–5 hours) or primary AML cells (right; $n = 3$; $t = 24$ hours; results for OCI-AML2 cells are shown in Supplementary Fig. S9) using the commercially available Amplite Fluorimetric Assay following treatment with avocatin B (10 μmol/L), palmitate (175 μmol/L), or avocatin B and palmitate according to the manufacturer's protocol. Data, percentage of NADH compared with vehicle control–treated cells ± SD.

for m/z 285 and 287 were nearly identical between pure compound and the cellular fractions (pure avocatin B: 4.46 and 4.76; mitochondrial fraction: 4.46 and 4.78; cytosolic fraction: 4.46 and 4.78). As expected, avocatin B was not found in vehicle control–treated cells (Supplementary Fig. S7).

Lipids of 16 to 20 carbon length enter mitochondria by the activity of CPT1 (32). To determine the role of CPT1 in avocatin B–induced death, we blocked CPT1 chemically with etomoxir and genetically using RNA interference. Etomoxir concentrations that did not reduce viability (100 μmol/L; Fig. 6A), abrogated avocatin B–induced cell death (Fig. 6B; $F_{5,17} = 94.45$; $P < 0.001$) and reductions in clonogenic growth (Fig. 6C; $F_{5,17} = 94.45$; $P < 0.001$). As a genetic approach, we generated cells with reduced CPT1 gene expression (mRNA: Fig. 6D, left; for protein see ref. 33). CPT1 knockdown cells were significantly less sensitive to avocatin B (Fig. 6D, middle; $F_{9,32} = 23.73$; $P < 0.001$) and were insensitive to avocatin B–induced reduction of NADPH (Fig. 6D, right; $F_{3,16} = 65.04$; $P < 0.001$). Together, these results show that avocatin B is a lipid that localizes to the mitochondria and impairs fatty acid oxidation.

Discussion

A screen of a natural health product library identified avocatin B as a novel anti-AML agent. *In vitro* and preclinical functional studies demonstrated that it induced selective toxicity toward leukemia and LSCs with no toxicity toward normal cells. Mechanistically, we highlight a novel strategy to induce selective leukemia cell death, where mitochondrial localization of avocatin B inhibits fatty acid oxidation and decreases levels of NADPH, resulting in elevated ROS leading to apoptotic cell death.

Avocatin B targets leukemia over normal cells. We propose this specificity is related to the leukemia cells' altered mitochondrial characteristics, as a number of observations suggest avocatin B targets mitochondria. For example, (i) we directly show avocatin B

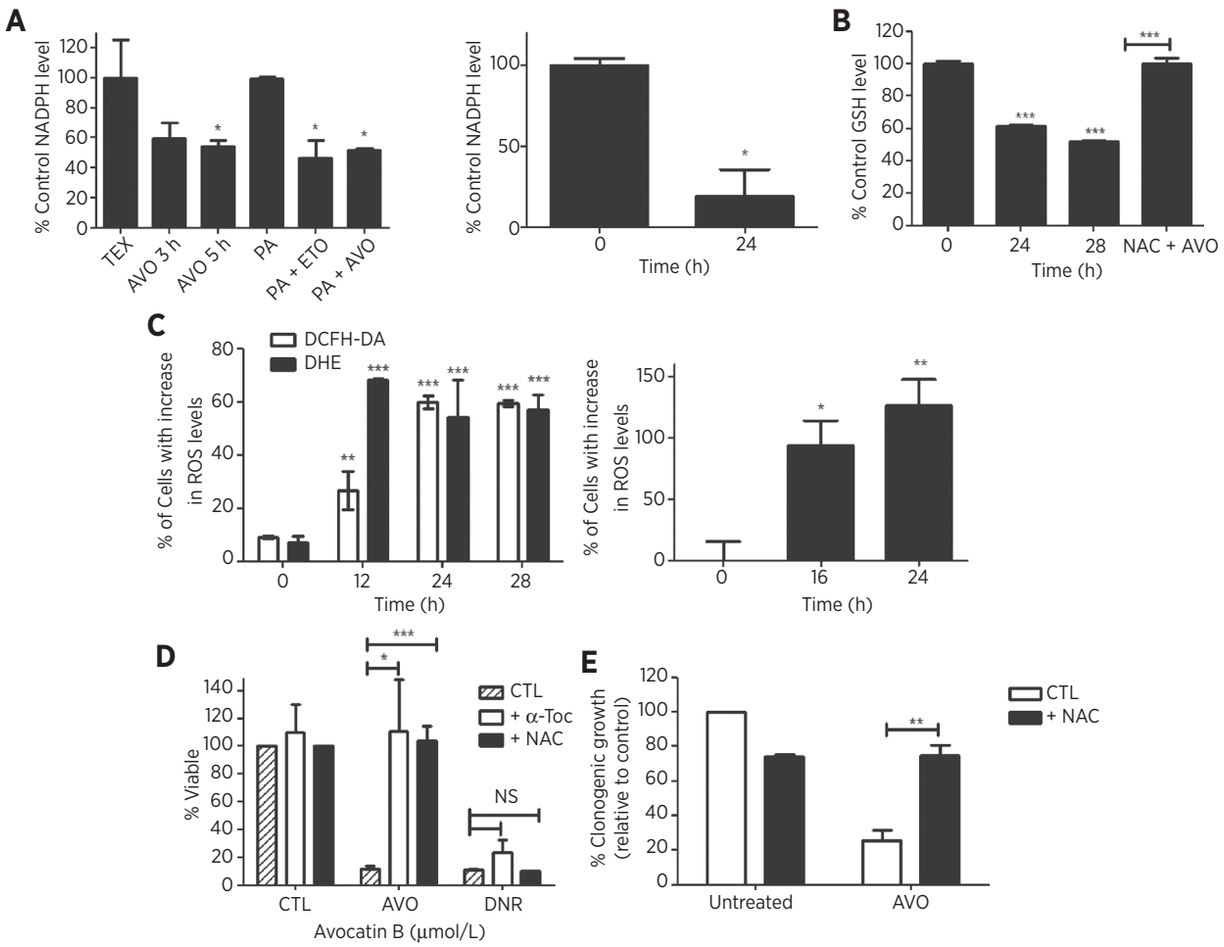

Figure 4.
Avocatin B decreased levels of NADPH and GSH and elevated ROS. A, NADPH was measured in TEX cells (left; $t = 3$–5 hours) or primary AML cells ($n = 3$; $t = 24$ hours, right; results for OCI-AML2 cells are shown in Supplementary Fig. S9) using the commercially available Amplite Fluorimetric Assay following treatment with avocatin B (10 μmol/L), palmitate (175 μmol/L), or etomoxir (100 μmol/L) according to the manufacturer's protocol. Data, a percentage of NADPH compared with vehicle control–treated cells ± SD. B, GSH was measured in TEX cells in the presence or absence of NAC using a commercially available fluorimetric assay following treatment with avocatin B (10 μmol/L), according to the manufacturer's protocol. Data, percentage of GSH compared with vehicle control–treated cells ± SD. C, ROS were measured in TEX cells (left) or primary AML cells ($n = 3$, right; results for OCI-AML2 cells is shown in Supplementary Fig. S9) treated with 10 μmol/L avocatin B for increasing time by DHE and DCFH-DA by flow cytometry. Data, percentage of cells with increased ROS compared with vehicle control ±SD from representative experiments. D, TEX cells were treated with 10 μmol/L avocatin B in the presence or absence of NAC or α-Toc, which can neutralize ROS. Daunorubicin (DNR) was used as a negative control. Viability was measured by the Annexin V/PI assay; data, mean percentage of viable cells (i.e., Annexin V^-/PI^-) ±SD from representative experiments. NS, nonsignificant. E, TEX cells were treated with 10 μmol/L avocatin B in the presence or absence of NAC and colonies were counted as described in Materials and Methods. All experiments were performed three times in triplicate, and representative figures are shown. *, $P < 0.05$; **, $P < 0.01$; ***, $P < 0.001$.

accumulates in leukemia cell mitochondria using LC/MS; (ii) cells with significantly reduced mitochondria or (iii) lacking the enzyme that facilitates mitochondrial lipid transport, CPT1, are insensitive to avocatin B; (iv) chemical treatment with etomoxir, a CPT1 inhibitor, blocked avocatin B's activity; and (v) CPT1 only facilitates entry of lipids of avocatin B's size into mitochondria [e.g., 16–20 carbons (32); avocatin B:17 carbons (21)]. Compared with normal hematopoietic cells, leukemia cells contain higher mitochondrial mass (1) and depend on fatty acid substrates for survival (2). Thus, given this mitochondrial phenotype, we propose that avocatin B accumulates with greater concentration in leukemia over normal cells, thus conferring its increased toxicity toward leukemia cells.

Inhibition of fatty acid oxidation by avocatin B resulted in ROS-induced apoptosis. Apoptosis was characterized by the mitochondrial proteins cytochrome *c* and AIF, which are commonly released following ROS-induced increases in mitochondrial outer membrane permeability (34, 35). Inhibiting fatty acid oxidation by blocking CPT1 with etomoxir resulted in ROS-dependent death of glioma cells caused by reduced concentrations of intracellular antioxidants attributed to decreased NADPH (26). Similarly, we demonstrated that avocatin B–induced inhibition of fatty acid oxidation decreased NADPH and GSH levels and that antioxidant supplementation rescued cells from death. NADPH is used for catabolic processes in proliferating cells and is able to regenerate cellular antioxidants (i.e., convert oxidized GSH,

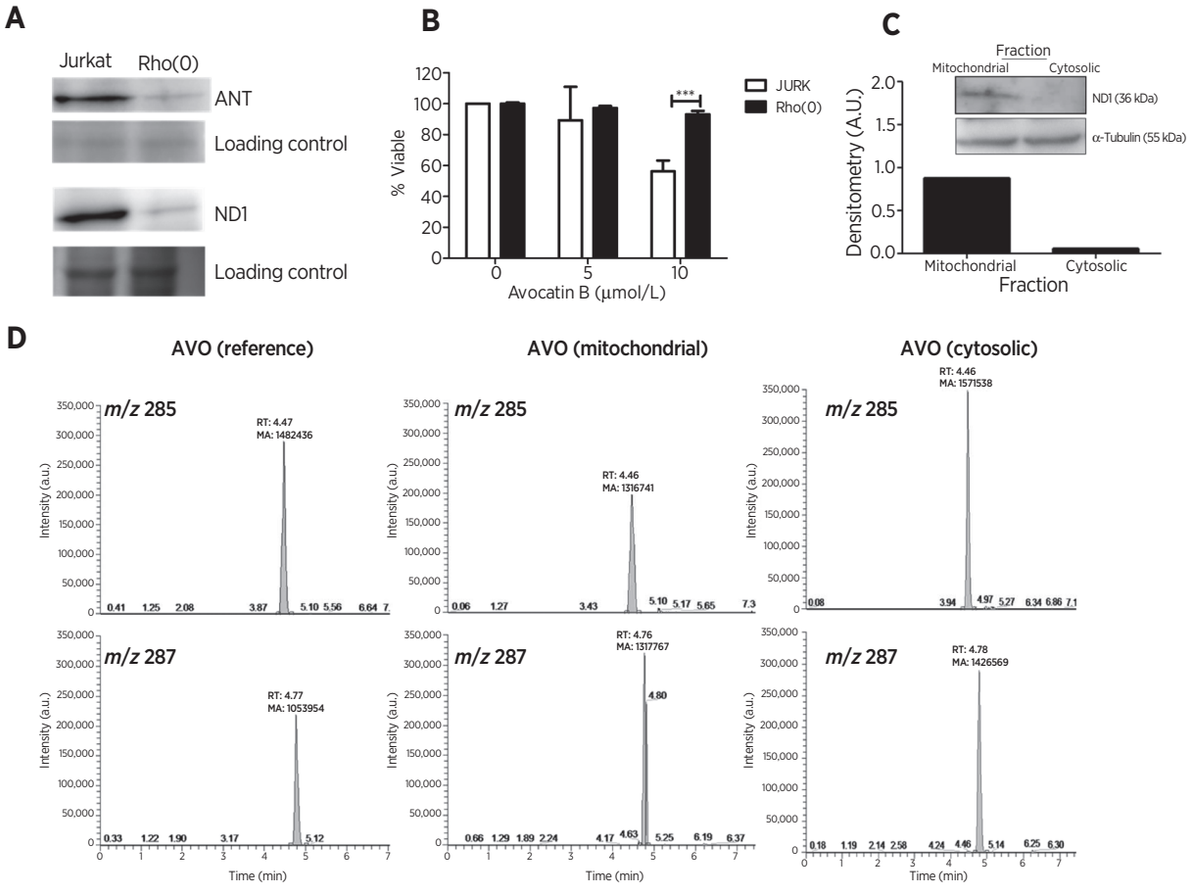

Figure 5.

Mitochondria are functionally important for avocatin B–induced death. A, Jurkat T cells were cultured in 50 ng/mL of ethidium bromide, 100 mg/mL sodium pyruvate, and 50 μg/mL uridine for 60 days to create Jurkat-Rho(0) cells, which lack functional mitochondrial. To confirm that Jurkat-Rho(0) cells lack mitochondria, we measured the mitochondria-specific markers ANT and complex I (ND1) by Western blotting. B, avocatin B's activity was tested in cells with (JURK) and with reduced [Jurkat-Rho(0)] mitochondria. Viability was measured by the Annexin V/PI assay and flow cytometry; data, mean percentage of live cells (i.e., Annexin V^-/PI^-) ±SD from representative experiments. C, mitochondrial and cytosolic fractions were collected, as outlined in Materials and Methods, and tested for purity by staining for the mitochondria-specific protein ND1. D, LC/MS chromatographs demonstrating the presence of avocatin B in the mitochondria and cytosol fractions of avocatin B–treated cells. All experiments were performed three times in triplicate, and representative figures are shown.
***, $P < 0.001$.

thioredoxins, and peroxiredoxins to their reduced equivalents), which counteract the detrimental effects of free radicals, including ROS; GSH specifically converts hydrogen peroxide to water (23, 36). Our observed NADPH decrease ($t = 5$ hours; Fig. 4A) preceded ROS elevation ($t = 12$ hours; Fig. 4C), further confirming the relationship between inhibition of fatty acid oxidation, NADPH, and ROS-dependent leukemia cell death. Of note, in our experiments, avocatin B accumulated in mitochondria to inhibit fatty acid oxidation and reduced NADPH at 10 μmol/L, whereas other studies used etomoxir, which blocks fatty acid entry into mitochondria and reduces NADPH at 100 μmol/L (2) or 1,000 μmol/L (26). Together, these results point to a mechanism in which avocatin B enters the mitochondria and potently inhibits fatty acid oxidation, resulting in decreased NADPH and GSH leading to elevated ROS and apoptotic cell death.

Avocatin B is a 1:1 ratio of two 17-carbon lipids derived from methanol extracted from avocado pear seeds (*Persea gratissima*; ref. 20). Odd-numbered carbons are rare, not produced endogenously and obtained only from dietary sources (37, 38). Moreover, they are not efficiently or preferentially oxidized. For example, mice fed diets containing radiolabeled odd- and even-numbered fatty acids only accumulate odd-numbered fatty acids in adipose tissue (i.e., C15 and 17; ref. 39); odd-numbered fatty acids show consistent adipose accumulation (37, 40, 41). In humans, lipids of 13, 15, and 17 carbon lengths are used as serum and adipose tissue biomarkers of dietary fat intake, as these fatty acids are more slowly catabolized compared with even-numbered fatty acids (38, 42). Although they undergo the same pathway of oxidation, the terminal step of odd-numbered fatty acid oxidation produces 1 acetyl-CoA and 1 propionyl-CoA molecule, whereas even-numbered fatty acids produce 2 acetyl-CoA molecules (43). Propionyl-CoA can then be converted to methylmalonyl-CoA by propinyl-CoA carboxylase and vitamin B12, at the expense of 1 ATP, which, in turn, is converted to succinyl-CoA that can enter the TCA cycle (41). Because this alternate pathway requires energy and delays overall ATP production, the decreased metabolic activity (i.e., reduced acetyl-CoA production and/or decreased entry of fatty acid byproducts into

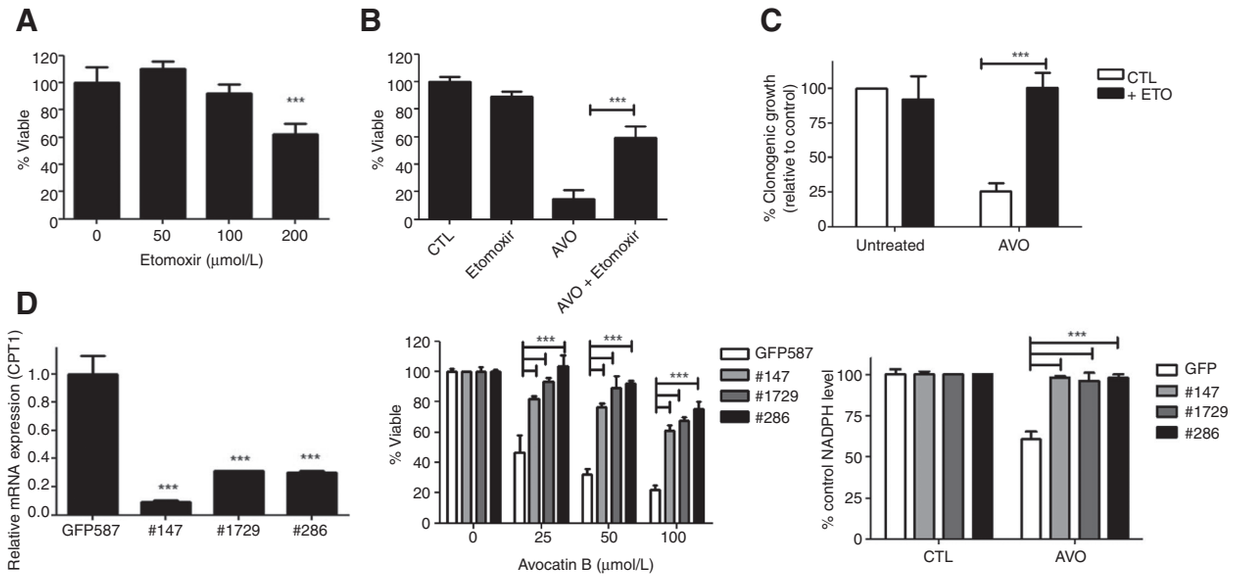

Figure 6.
CPT1 is functionally important for avocatin B–induced death. A, TEX cells were incubated with increasing concentrations of the CPT1 inhibitor etomoxir for 72 hours. B and C, avocatin B's (10 μmol/L) activity was tested using Annexin V/PI (B) or colony assays (C) in the presence of etomoxir (100 μmol/L; which does not impart toxicity). D, left, mRNA expression demonstrating knockdown of CPT1 in OCI-AML2 cells. Middle, avocatin B's activity was tested in CPT1 knockout cells. Right, NADPH was tested in CPT1 knockout cells following avocatin B (10 μmol/L) treatment. Data, percentage of NADPH relative to control. Unless otherwise noted, viability was measured by the Annexin V/PI assay and flow cytometry; data, mean percentage of live cells (i.e., Annexin V^-/PI^-) ±SD from representative experiments. All experiments were performed three times in triplicate, and representative figures are shown. ***, $P < 0.001$.

the TCA cycle) likely explains our observed decrease in NAD and NADPH. As such, decreased levels of NADPH may not only result in elevated ROS, but also indicate a decrease in overall metabolic activity. Thus, a novel pathway by which fatty acid oxidation can be inhibited in leukemia cells is by the odd-numbered carbon lipid, avocatin B stalling or rendering less efficient the fatty acid oxidation pathway. This highlights a novel strategy to induce selective leukemia cell death by which preferential mitochondrial localization of avocatin B reduces leukemia cell metabolism and decreases NADPH, leading to ROS-mediated cell death.

Alternatively, mitochondrial accumulation of fatty acids could have lipotoxic effects. When in excess, fatty acids can accumulate inside the mitochondrial matrix where they are deprotonated, because of the proton gradient, creating fatty acid anions. These are converted by ROS into lipid peroxides that, in turn, cause damage to mitochondrial DNA, lipids, and proteins within the mitochondrial matrix (44). However, the generation of lipotoxic products requires ROS (45), therefore; avocatin B accumulation by itself would be insufficient to impart lipotoxicity. Thus, once inside the mitochondria, avocatin B or avocatin B derivatives may be converted to lipotoxic byproducts and contribute to death but only after sufficient ROS production (i.e., following avocatin B–induced inhibition of fatty acid oxidation). Thus, mitochondrial accumulation may contribute to death through lipotoxicity but this is not the underlying mechanism of avocatin B's activity.

Few compounds that inhibit fatty acid oxidation are currently approved for clinical use (23). CPT1 inhibitors, such as etomoxir and perhexiline, are associated with hepatoxicity (46) and neurotoxicity (47), respectively, and are not approved for clinical use in North America. Other inhibitors, such as trimetazidine, which inhibits 3-ketoacyl-CoA thiolase, an enzyme involved in fatty acid catabolism and ranolazine, which blocks late sodium currents, have had clinical success for the treatment of angina (48, 49). None of these compounds are approved for use in AML or other hematologic malignancies. Future studies are needed to asses avocatin B's pharmacology and pharmacokinetics; however, initial assessment of avocatin B's physicochemical properties suggests favorable tissue distribution. In particular, it possesses a high estimated partition coefficient (LogP = 8.9; ref. 21), indicating that it will accumulate in lipid-rich tissues such as adipose tissue and bone marrow. Given that LSCs reside in bone marrow, this could significantly enhance avocatin B's therapeutic efficacy. Nonetheless, future studies are needed to test the pharmacokinetics and safety of avocatin B in human trials.

In conclusion, avocatin B accumulated in mitochondria to inhibit fatty acid oxidation and decrease NADPH, resulting in ROS-mediated cell death characterized by the mitochondrial release of cytochrome *c* and AIF. Given the observed leukemia cell specificity, inhibiting fatty acid oxidation following avocatin B accumulation represents a novel therapeutic strategy that targets an important cellular pathway involved in leukemia cell activity.

Disclosure of Potential Conflicts of Interest

No potential conflicts of interest were disclosed.

Authors' Contributions

Conception and design: E.A. Lee, J.W. Joseph, A.D. Schimmer, P.A. Spagnuolo
Development of methodology: E.A. Lee, E. Boyaci, B. Bojko, S. Sriskanthadevan, J. Pawliszyn, J.W. Joseph, P.A. Spagnuolo
Acquisition of data (provided animals, acquired and managed patients, provided facilities, etc.): E.A. Lee, L. Angka, S.-G. Rota, T. Hanlon, A. Mitchell, X.M. Wang, M. Minden, A. Datti, J.L. Wrana, J.W. Joseph, J. Quadrilatero, P.A. Spagnuolo

Analysis and interpretation of data (e.g., statistical analysis, biostatistics, computational analysis): E.A. Lee, L. Angka, S.-G. Rota, A. Mitchell, E. Boyaci, A. Datti, J. Pawliszyn, J.W. Joseph, J. Quadrilatero, P.A. Spagnuolo
Writing, review, and/or revision of the manuscript: E.A. Lee, L. Angka, M. Gronda, M. Minden, A. Edginton, J.W. Joseph, A.D. Schimmer, P.A. Spagnuolo
Administrative, technical, or material support (i.e., reporting or organizing data, constructing databases): E.A. Lee, R. Hurren, M. Gronda, A.D. Schimmer, P.A. Spagnuolo
Study supervision: A.D. Schimmer, P.A. Spagnuolo

Acknowledgments

The authors thank Dr. John Dick for the generous gift of TEX cells.

Grant Support

This study was supported by grants from the Leukemia & Lymphoma Society of Canada and University of Waterloo (P.A. Spagnuolo); the Natural Sciences and Engineering Research Council of Canada (J. Quadrilatero and J. Pawliszyn); and the Canadian Institutes of Health Research (J.W. Joseph). A.D. Schimmer is a Leukemia and Lymphoma Society Scholar in Clinical Research.

The costs of publication of this article were defrayed in part by the payment of page charges. This article must therefore be hereby marked *advertisement* in accordance with 18 U.S.C. Section 1734 solely to indicate this fact.

Received September 11, 2014; revised March 17, 2015; accepted April 2, 2015; published online June 15, 2015.

References

1. Skrtic M, Sriskanthadevan S, Jhas B, Gebbia M, Wang X, Wang Z, et al. Inhibition of mitochondrial translation as a therapeutic strategy for human acute myeloid leukemia. Cancer Cell 2011;20:674–88.
2. Samudio I, Harmancey R, Fiegl M, Kantarjian H, Konopleva M, Korchin B, et al. Pharmacologic inhibition of fatty acid oxidation sensitizes human leukemia cells to apoptosis induction. J Clin Invest 2010;120:142–56.
3. Shipley JL, Butera JN. Acute myelogenous leukemia. Exp Hematol 2009; 37:649–58.
4. Lowenberg B, Downing JR, Burnett A. Acute myeloid leukemia. N Engl J Med 1999;341:1051–62.
5. McDermott SP, Eppert K, Notta F, Isaac M, Datti A, Al-Awar R, et al. A small molecule screening strategy with validation on human leukemia stem cells uncovers the therapeutic efficacy of kinetin riboside. Blood 2012;119: 1200–7.
6. Spagnuolo PA, Hurren R, Gronda M, MacLean N, Datti A, Basheer A, et al. Inhibition of intracellular dipeptidyl peptidases 8 and 9 enhances parthenolide's anti-leukemic activity. Leukemia 2013;27:1236–44.
7. Spagnuolo PA, Hu J, Hurren R, Wang X, Gronda M, Sukhai MA, et al. The antihelmintic flubendazole inhibits microtubule function through a mechanism distinct from Vinca alkaloids and displays preclinical activity in leukemia and myeloma. Blood 2010;115:4824–33.
8. Sukhai MA, Prabha S, Hurren R, Rutledge AC, Lee AY, Sriskanthadevan S, et al. Lysosomal disruption preferentially targets acute myeloid leukemia cells and progenitors. J Clin Invest 2013;123:315–28.
9. Sachlos E, Risueno RM, Laronde S, Shapovalova Z, Lee JH, Russell J, et al. Identification of drugs including a dopamine receptor antagonist that selectively target cancer stem cells. Cell 2012;149:1284–97.
10. Angka L, Lee EA, Rota SG, Hanlon T, Sukhai M, Minden M, et al. Glucopsychosine increases cytosolic calcium to induce calpain-mediated apoptosis of acute myeloid leukemia cells. Cancer Lett 2014;348:29–37.
11. Abe Y, Sakairi T, Beeson C, Kopp JB. TGF-beta1 stimulates mitochondrial oxidative phosphorylation and generation of reactive oxygen species in cultured mouse podocytes, mediated in part by the mTOR pathway. Am J Physiol Renal Physiol 2013;305:F1477–90.
12. Dam AD, Mitchell AS, Rush JW, Quadrilatero J. Elevated skeletal muscle apoptotic signaling following glutathione depletion. Apoptosis 2012;17: 48–60.
13. Owusu-Ansah E, Yavari A, Banerjee U. A protocol for *in vivo* detection of reactive oxygen species. 2008; doi:10.1038/nprot.2008.23.
14. Boyaci E, Sparham C, Pawliszyn J. Thin-film microextraction coupled to LC-ESI-MS/MS for determination of quaternary ammonium compounds in water samples. Anal Bioanal Chem 2014;406:409–20.
15. Boyaci E, Gorynski K, Rodriguez-Lafuente A, Bojko B, Pawliszyn J. Introduction of solid-phase microextraction as a high-throughput sample preparation tool in laboratory analysis of prohibited substances. Anal Chim Acta 2014;809:69–81.
16. McMillan EM, Graham DA, Rush JW, Quadrilatero J. Decreased DNA fragmentation and apoptotic signaling in soleus muscle of hypertensive rats following 6 weeks of treadmill training. J Appl Physiol 2012;113: 1048–57.
17. Christensen ME, Jansen ES, Sanchez W, Waterhouse NJ. Flow cytometry based assays for the measurement of apoptosis-associated mitochondrial membrane depolarisation and cytochrome c release. Methods 2013;61: 138–45.
18. Waterhouse NJ, Trapani JA. A new quantitative assay for cytochrome c release in apoptotic cells. Cell Death Differ 2003;10:853–5.
19. Warner JK, Wang JC, Takenaka K, Doulatov S, McKenzie JL, Harrington L, et al. Direct evidence for cooperating genetic events in the leukemic transformation of normal human hematopoietic cells. Leukemia 2005;19: 1794–805.
20. Alves HM, Coxon DT, Falshaw CP, Godtfredsen WO, Ollis WD. The Avocatins—a new class of natural products. Ann Braz Acad Sci 1970;42:4.
21. ChemBank. 2014; Cited Sept 2014. http://chembank.broadinstitute.org/chemistry/viewMolecule.htm;jsessionid=9CC037B2065BFDE714299282-DD50A255?cbid=3198534.
22. Konopleva M, Watt J, Contractor R, et al. Mechanisms of antileukemic activity of the novel Bcl-2 homology domain-3 mimetic GX15-070 (obatoclax). Cancer Res 2008;68:3413–20.
23. Carracedo A, Cantley LC, Pandolfi PP. Cancer metabolism: fatty acid oxidation in the limelight. Nat Rev Cancer 2013;13:227–32.
24. Heiden MGV, Cantley LC, Thompson CB. Understanding the Warburg effect: the metabolic requirements of cell proliferation. Science 2009;324: 1029–33.
25. Kirsch M, De Groot H. NAD(P)H, a directly operating antioxidant? FASEB J 2001;15:1569–74.
26. Pike LS, Smift AL, Croteau NJ, Ferrick DA, Wu M. Inhibition of fatty acid oxidation by etomoxir impairs NADPH production and increases reactive oxygen species resulting in ATP depletion and cell death in human glioblastoma cells. Biochim Biophys Acta 2011;1807: 726–34.
27. Godbout JP, Berg BM, Kelley KW, Johnson RW. alpha-Tocopherol reduces lipopolysaccharide-induced peroxide radical formation and interleukin-6 secretion in primary murine microglia and in brain. J Neuroimmunol 2004;149:101–9.
28. Ferraro C, Quemeneur L, Prigent AF, Taverne C, Revillard JP, Bonnefoy-Berard N. Anthracyclines trigger apoptosis of both G_0-G_1 and cycling peripheral blood lymphocytes and induce massive deletion of mature T and B cells. Cancer Res 2000;60:1901–7.
29. Vejpongsa P, Yeh ETH. Topoisomerase 2 beta: a promising molecular target for primary prevention of anthracycline-induced cardiotoxicity. Clin Pharmacol Ther 2014;95:45–52.
30. Desjardins P, Frost E, Morais R. Ethidium bromide-induced loss of mitochondrial DNA from primary chicken embryo fibroblasts. Mol Cell Biol 1985;5:1163–9.
31. Hashiguchi K, Zhang-Akiyama QM. Establishment of human cell lines lacking mitochondrial DNA. Methods Mol Biol 2009;554: 383–91.
32. Reddy JK, Hashimoto T. Peroxisomal beta-oxidation and peroxisome proliferator-activated receptor alpha: an adaptive metabolic system. Annu Rev Nutr 2001;21:193–230.
33. Sriskanthadevan S, Jeyaraju DV, Chung TE, Prabha S, Xu W, Skrtic M, et al. AML cells have low spare reserve capacity in their respiratory chain that renders them susceptible to oxidative metabolic stress. Blood 2015;125: 2120–30.
34. Tomasello F, Messina A, Lartigue L, Schembri L, Medina C, Reina S, et al. Outer membrane VDAC1 controls permeability transition of the inner mitochondrial membrane in cellulo during stress-induced apoptosis. Cell Res 2009;19:1363–76.

35. Kroemer G, Galluzzi L, Brenner C. Mitochondrial membrane permeabilization in cell death. Physiol Rev 2007;87:99–163.
36. Vander Heiden MG, Cantley LC, Thompson CB. Understanding the Warburg effect: the metabolic requirements of cell proliferation. Science 2009;324:1029–33.
37. Campbell RG, Hashim SA. Deposition in adipose tissue and transport of odd-numbered fatty acids. Am J Physiol 1969;217:1614–8.
38. Wolk A, Furuheim M, Vessby B. Fatty acid composition of adipose tissue and serum lipids are valid biological markers of dairy fat intake in men. J Nutr 2001;131:828–33.
39. Gotoh N, Moroda K, Watanabe H, Yoshinaga K, Tanaka M, Mizobe H, et al. Metabolism of odd-numbered fatty acids and even-numbered fatty acids in mouse. J Oleo Sci 2008;57:293–9.
40. Pi-Sunyer FX. Rats enriched with odd-carbon fatty acids. Effect of prolonged starvation on liver glycogen and serum lipids, glucose and insulin. Diabetes 1971;20:200–5.
41. VanItallie TB, Khachadurian AK. Rats enriched with odd-carbon fatty acids: maintenance of liver glycogen during starvation. Science 1969; 165:811–3.
42. Klein RA, Halliday D, Pittet PG. The use of 13-methyltetradecanoic acid as an indicator of adipose tissue turnover. Lipids 1980;15:572–9.
43. Berg JM, Tymoczko JL, Stryer L. Biochemistry. Certain fatty acids require additional steps for degradation. 5th ed. New York: W H Freeman; 2002. Available from: http://www.ncbi.nlm.nih.gov/books/NBK22387/.
44. Schrauwen P, Hesselink MK. Oxidative capacity, lipotoxicity, and mitochondrial damage in type 2 diabetes. Diabetes 2004;53:1412–7.
45. Schrauwen P, Schrauwen-Hinderling V, Hoeks J, Hesselink MK. Mitochondrial dysfunction and lipotoxicity. Biochim Biophys Acta 2010;1801: 266–71.
46. Holubarsch CJ, Rohrbach M, Karrasch M, Boehm E, Polonski L, Ponikowski P, et al. A double-blind randomized multicentre clinical trial to evaluate the efficacy and safety of two doses of etomoxir in comparison with placebo in patients with moderate congestive heart failure: the ERGO (etomoxir for the recovery of glucose oxidation) study. Clin Sci 2007;113:205–12.
47. Ashrafian H, Horowitz JD, Frenneaux MP. Perhexiline. Cardiovasc Drug Rev 2007;25:76–97.
48. Passeron J. [Effectiveness of trimetazidine in stable effort angina due to chronic coronary insufficiency. A double-blind versus placebo study]. Presse Med 1986;15:1775–8.
49. Aldakkak M, Stowe DF, Camara AK. Safety and efficacy of ranolazine for the treatment of chronic angina pectoris. Clin Med Insights Ther 2013;2013: 1–14.

Targeting Mitochondria with Avocatin B Induces Selective Leukemia Cell Death

Eric A. Lee, Leonard Angka, Sarah-Grace Rota, et al.

Cancer Res 2015;75:2478-2488.